

Dynamic Phasor Model of Grid-Connected Photovoltaic System in MATLAB/Simulink Considering Low Voltage Ride through Characteristics for Voltage Stability Analysis of Power System

Tien Luan Dinh, Hoang Viet Nguyen*, Quoc Viet Hoang, Minh Truong Ngoc
Hanoi University of Science and Technology, Hanoi, Vietnam
*Email: viet.nguyenhoang1@hust.edu.vn

Abstract

This paper proposes a model of grid-connected photovoltaic (PV) system with low voltage ride through (LVRT) characteristic in MATLAB/Simulink based on dynamic phasor approach. Unlike all PV system models available in MATLAB/Simulink using detailed model with small capacity, the proposed model focuses on control loops of PV system to simulate a large capacity system that is appropriate for voltage stability analysis of power system installing high penetration level of PV generation. An intuitive and convenient tool for adjusting the LVRT characteristics of the PV system is also developed. The effectiveness of dynamic phasor model and the impact of the LVRT characteristic of the PV system on voltage stability are examined through MATLAB/Simulink simulations conducted on IEEE 9-bus test system. The simulation results provide an insight of how the system integrated with a large PV generation behaves under the disturbances. It also points out that the LVRT of the PV system is very important to the power system voltage stability.

Keywords: Photovoltaic (PV), renewable energy, low voltage ride through (LVRT), voltage stability, MATLAB/simulink.

1. Introduction

The rapid development of solar power using photovoltaic (PV) technology has great significance in addressing energy needs and environmental protection. However, the disadvantage of PV is the uncertainty of the primary energy source, causing the output power to change respectively. Therefore, the connection of solar power to the grid can affect many aspects of the system operation and stability [1], [2]. When solar power plants are connected to the grid, they must comply with the low voltage ride through (LVRT) characteristic. This feature requires the plant to maintain connection for a certain period when disturbances occur. The duration that the plants can stay connected has a great influence on the stability of the system. So, there is a need for studies on the design and connection of power plants. Convenient and fast simulation tools are necessary for analyzing the above problems.

This paper introduces a dynamic phasor model of PV system built in MATLAB/Simulink. The phasor type of simulation method available in Simulink is commonly used for studying electromechanical oscillations of power systems consisting of a large number of generators and motors. This method computes voltage and current, in which complex numbers representing sinusoidal voltages and currents are expressed either in Cartesian coordinates or in polar coordinates (amplitude and phase). Therefore,

simulation can be performed much faster and is appropriate for power system stability analysis [2]-[5]. However, dynamic phasor models in [3]-[5] are not used for PV systems and research [2] only focuses on transient stability.

The PV system modelling in this paper can be used for analyzing and controlling voltage stability of the power system. The model does not simulate PV arrays or small capacity DC/DC converters and DC/AC inverters in detail but targets the control system of the PV system and P-V curve of PV arrays to simulate large capacity systems and be suitable for voltage stability research. The paper also develops a tool that is able to adjust the LVRT characteristic in a convenient way. The proposed model is applied for analyzing voltage stability of IEEE 9-bus grid installing high penetration level of PV system in several different scenarios.

This paper is organized as follows. Section 2 introduces the basic knowledge about dynamic phasor. The structure and model of grid-connected PV system and the LVRT characteristic are presented in Section 3. Simulation results are shown in Section 4 and conclusions are presented in Section 5.

2. Introduction to the Dynamic Phasor

Continuous mode, discrete, phasor are the three modes used for simulating power system in MATLAB/Simulink. Fig. 1 represents the differences

of three modes in representing voltage in time domain. Continuous mode is a very precise simulation mode with continuous computation steps. Discrete mode uses fixed calculation steps, so it performs fewer calculations than continuous mode, and simulation results depend on the chosen calculation step value, and in some cases, the results may not be calculated correctly. Compared with the two proposed methods, the phasor simulation mode stands out for its fast calculation speed, and it is used in the research model. This method uses a set of simple algebraic equations involving voltage and current phasors. Phasors are complex numbers that represent sinusoidal voltages and currents at a particular frequency. They can be represented either in Cartesian coordinate system or in polar coordinate system. The mathematical representation of the phasor is shown below.

Representation of any periodic waveform in complex Fourier coefficients is given in the following:

$$x(\tau) = \sum_{k=-\infty}^{\infty} \langle x \rangle_k e^{jk\omega_0\tau} \quad (1)$$

where $\omega_0 = \frac{2\pi}{T}$ and $\langle x \rangle_k$ represents the k^{th} dynamic phasor of the signal [4] and it can be computed as follows:

$$\langle x \rangle_k(t) = \frac{1}{T} \int_{t-T}^t x(\tau) e^{-jk\omega_0\tau} d\tau \quad (2)$$

Important properties of dynamic phasors [5] are:

- 1) The derivation of the dynamic phasor is given by:

$$\frac{d\langle x \rangle_k}{dt} = \left(\frac{dx}{dt} \right)_k - jk\omega_0 X_k \quad (3)$$

- 2) Product of dynamic phasors:

The k^{th} phasor of the product of two waveforms $u(t)$ and $v(t)$ can be obtained by the discrete convolution of the corresponding dynamic phasors as follows:

$$\langle uv \rangle_k = \sum_{l=-\infty}^{\infty} \langle u \rangle_{k-l} \langle v \rangle_l \quad (4)$$

- 3) For a real valued signal $x(\tau)$, the relationship between $\langle x \rangle_k$ and $\langle x \rangle_{-k}$ is given as:

$$\langle x \rangle_{-k} = \langle x \rangle_k^* \quad (5)$$

where $\langle x \rangle_k^*$ means the complex conjugate of $\langle x \rangle_k$.

3. Structure and Model of Grid-Connected PV

PV system structure consists of PV panels, DC/DC converter, DC/AC inverter, grid-connected L filter and control systems as shown in Fig. 2 [6]. The simplified model of elements and controllers built in MALAB/Simulink can be seen in Fig. 3.

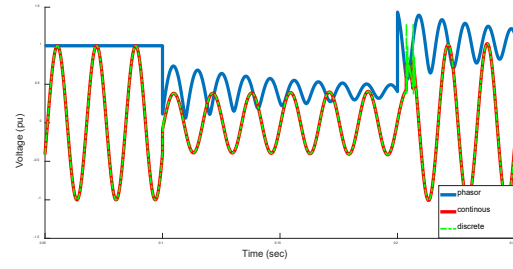


Fig. 1. Voltage lines in three simulation modes

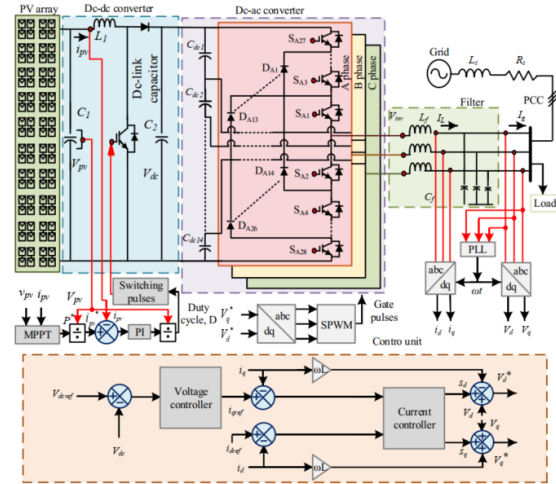


Fig. 2. Grid-connected PV system structure

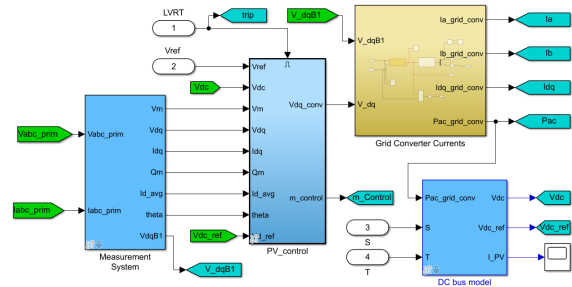


Fig. 3. PV control system

3.1. PV Panel Modelling

The simplified model of PV panel [7], [8] are simulated at standard conditions ($S_{ref} = 1000 \text{ W/m}^2$, $T_{ref} = 25^\circ\text{C}$), four typical parameters of the panels are short circuit current I_{scref} , open circuit voltage U_{ocref} , current and voltage at the peak powerpoint I_{mref} , U_{mref} . Under other conditions, the output current of the panel is represented by:

$$I = I_{sc} \left[1 - C_1 \left(e^{\frac{U}{C_2 U_{oc}}} - 1 \right) \right] \quad (6)$$

where:

$$\begin{cases} C_1 = (1 - I_{mref}/I_{scref}) e^{-U_{mref}/(C_2 U_{ocref})} \\ C_2 = (U_{mref}/U_{ocref} - 1) / [\ln(1 - I_{mref}/I_{scref})] \end{cases}$$

3.2. Inverter Modelling

The inverter of grid-connected PV system has significant role in transferring power from PV system to the grid. The grid-connected inverter which is shown in Fig. 4 [9] is usually controlled to keep both the active power and the reactive power at the reference set points [9]-[13]. The control objective is also to make sure that DC voltage can be adjusted. In addition to the voltage and frequency requirements at the output of the converter, the output current also needs to be in sinusoidal form and less affected by harmonics. To facilitate the design and calculation of control variables based on dynamic phasor model, three-phase quantities (voltage, current, etc.) are transformed to longitudinal and transverse components in the direct-quadrature-zero ($dq0$) rotating reference frame. The amount of computational equation system can be reduced, and the calculating of control variables becomes easier.

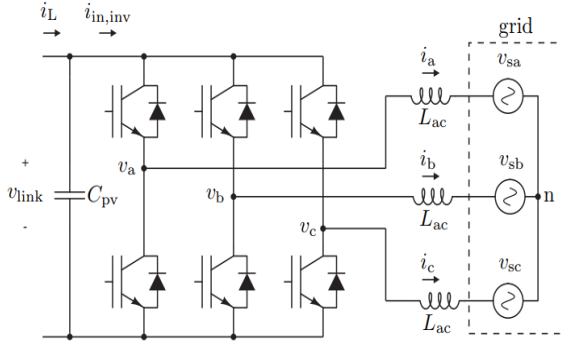


Fig. 4. Grid-connected inverter structure

3.2.1. The $dq0$ Rotating Reference Frame

The three-phase signals are converted to the $dq0$ rotating reference frame shown in Fig. 5 based on the Park transformation:

$$[x_{dq0}] = T[\varepsilon(t)][x_{abc}] \quad (7)$$

where $T[\varepsilon(t)]$ equals to:

$$\frac{2}{3} \begin{bmatrix} \cos[\varepsilon(t)] & \cos\left[\varepsilon(t) - \frac{2\pi}{3}\right] & \cos\left[\varepsilon(t) - \frac{4\pi}{3}\right] \\ \sin[\varepsilon(t)] & \sin\left[\varepsilon(t) - \frac{2\pi}{3}\right] & \sin\left[\varepsilon(t) - \frac{4\pi}{3}\right] \\ \frac{1}{2} & \frac{1}{2} & \frac{1}{2} \end{bmatrix}$$

Using Park transformation, voltage and current becomes:

$$\begin{cases} \vec{v}(t) = (v_d + jv_q)e^{j\varepsilon(t)} \\ \vec{i}^*(t) = (i_d - ji_q)e^{-j\varepsilon(t)} \end{cases} \quad (8)$$

Then, the active and reactive power is expressed as follows:

$$P(t) = \frac{3}{2} [v_d(t)i_d(t) + v_q(t)i_q(t)] \quad (9)$$

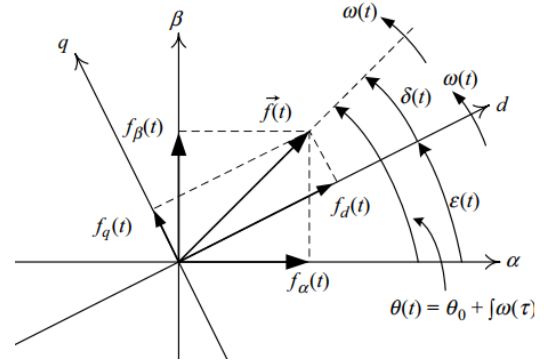


Fig. 5. The $dq0$ and $\alpha\beta$ rotating reference frame

$$Q(t) = \frac{3}{2} [-v_d(t)i_q(t) + v_q(t)i_d(t)] \quad (10)$$

Based on (9) and (10), if $v_q = 0$, to control the output active power and reactive power of PV, only two quantities i_d , i_q are needed to be controlled. This property is widely used in the control of grid-connected three-phase inverter control systems.

3.2.2. Voltage Control Loop

In most grid-connected inverters, a capacitor between the PV arrays and the DC/AC inverter is needed to ensure a balance between the input and output power of the inverter. The DC voltage on capacitor is kept staying unchanged, in order to keep the power transferred to the grid stable.

The larger the power converts, the higher the amplitude of the grid current is. Therefore, it is necessary to control the capacity of the DC/AC inverter to control DC voltage. The DC voltage needs to be maintained stably in the PV system and controlled at the desired value. The power passing through the capacitor can be changed through the DC voltage control to ensure power balance.

$$\begin{cases} P_{DC} = v_{DC}i_{DC} - v_{DC}C_{DC}\frac{dv_{DC}}{dt} \\ P_{AC} = \frac{3}{2}(v_d i_d + v_q i_q) \end{cases} \quad (11)$$

In the calculation, simulation, it is assumed that the power loss in the inverter is ignored, the input and output power of the inverter is the same, it means that:

$$v_{DC}i_{DC} - v_{DC}C_{DC}\frac{dv_{DC}}{dt} = \frac{3}{2}(v_d i_d + v_q i_q) \quad (12)$$

$$\begin{aligned} v_{DC}(s) &= G_{p-DC}(s)i_d(s) \\ &= \frac{3}{2} \frac{V_m}{I_{DC} - sC_{DC}V_{DC}} i_d(s) \end{aligned} \quad (13)$$

For the convenience of designing controller, consider $v_d = V_m$ and $v_q = 0$. Then, the DC voltage control loop is represented as in Fig. 6.

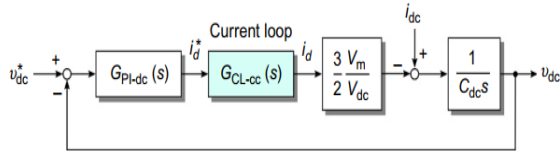


Fig. 6. Voltage control loop

3.2.3. Current Control Loop

The main task of the current controller is to regulate the current by generating the appropriate output voltage. According to Fig. 4, based on Kirchhoff's law, the current at the output of the DC/AC inverter in the $dq0$ coordinate system is represented as follow:

$$\begin{cases} L \frac{di_d}{dt} + Ri_d - \omega Li_q = v_{d1} - v_d \\ L \frac{di_q}{dt} + Ri_q + \omega Li_d = v_{q1} - v_q \end{cases} \quad (14)$$

where i_d and i_q are output currents of the inverter in $dq0$ reference frame; v_{d1} , v_{q1} are converted voltages on d -axis and q -axis; v_d , v_q are output voltages of the L filter, ω is system angular frequency.

The output currents i_d and i_q modulation is shown in Fig. 7. It can be seen that the reference voltage-to-current inverter block on the $dq0$ reference frame is the same. Therefore, the inverter only needs to design one PI controller for both outputs based on the following equation.

$$\frac{i_d(s)}{v_{d1}^*(s)} = \frac{i_q(s)}{v_{q1}^*(s)} = \frac{1}{Ls + R} \quad (15)$$

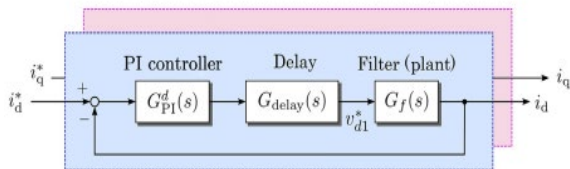


Fig. 7. Current control loop

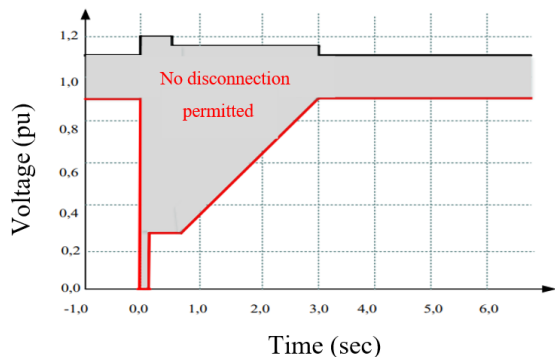


Fig. 8. LVRT characteristic of Vietnam

3.2.4. LVRT Characteristic

LVRT capability represents the most important technical requirement for PV inverters with regard to

system security. LVRT generally means that a generator is not allowed to disconnect in the case of a short-term voltage dip resulting from a short-circuit in the grid. This characteristic is typically specified by a curve which represents the lower limit of voltage vs. time for which no disconnection is permitted. An example of LVRT curve is shown in Fig. 8 [14]. When the voltage curve cuts the LVRT curve, PV is disconnected due to the operation of the switching control system that is integrated in the built model.

4. Simulation and Results

The PV system is connected to a 3-machine 9-bus system at the middle of the lines 5-7 through a transformer 24.5/230 kV, this system is shown in Fig. 11. The power output of the PV system is 130 MW accounting for 40% of the total system demand. The parameters of the PV system as shown in Table 1.

Table 1. Parameter values

Parameters	Values	Control Coefficients	Values
U_m/V	54.7	$k_{p,v}$	0.89
I_m/A	5.76	$k_{i,v}$	887.50
U_{oc}/V	64.6	$k_{p,I}$	25.10
I_{sc}/A	6.14	$k_{i,I}$	0.25
$C_{dc}/\mu F$	793.8	f_s/kHz	5
L_f/mH	15.1		

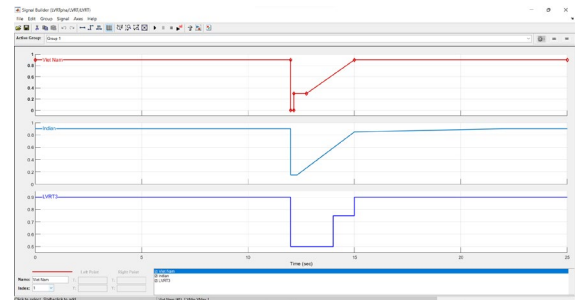


Fig. 9. Design LVRT in Signal Builder

To study the impacts of LVRT characteristics, in this paper, a 3-phase short circuit is applied at bus 7 for a period of 0.1s, 0.2s, 0.3s, 0.4s from the 12th second with gird code of Vietnam and India (VIE-LVRT and IND-LVRT respectively). The LVRT characteristics are built intuitively based on the Signal Builder block in Simulink as shown in Fig. 9, these characteristic curves can be modified easily by simple manipulation in MATLAB/Simulink windows.

At the initial stage, the simulated voltage and power values of the panels (Fig. 10) reach stable values quickly, with low spikes, showing that the control system has a high response and is suitable for research purposes.

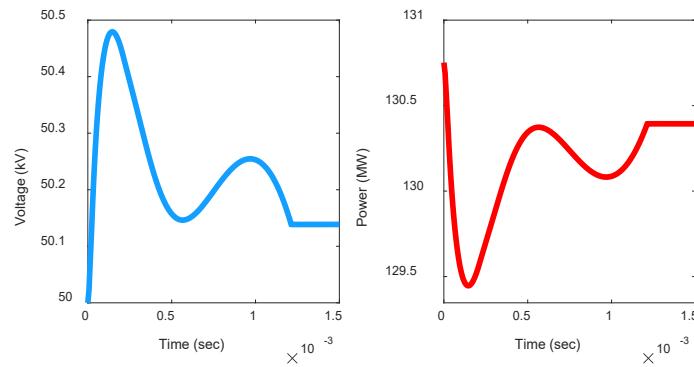


Fig. 10. Voltage and power characteristic of PV

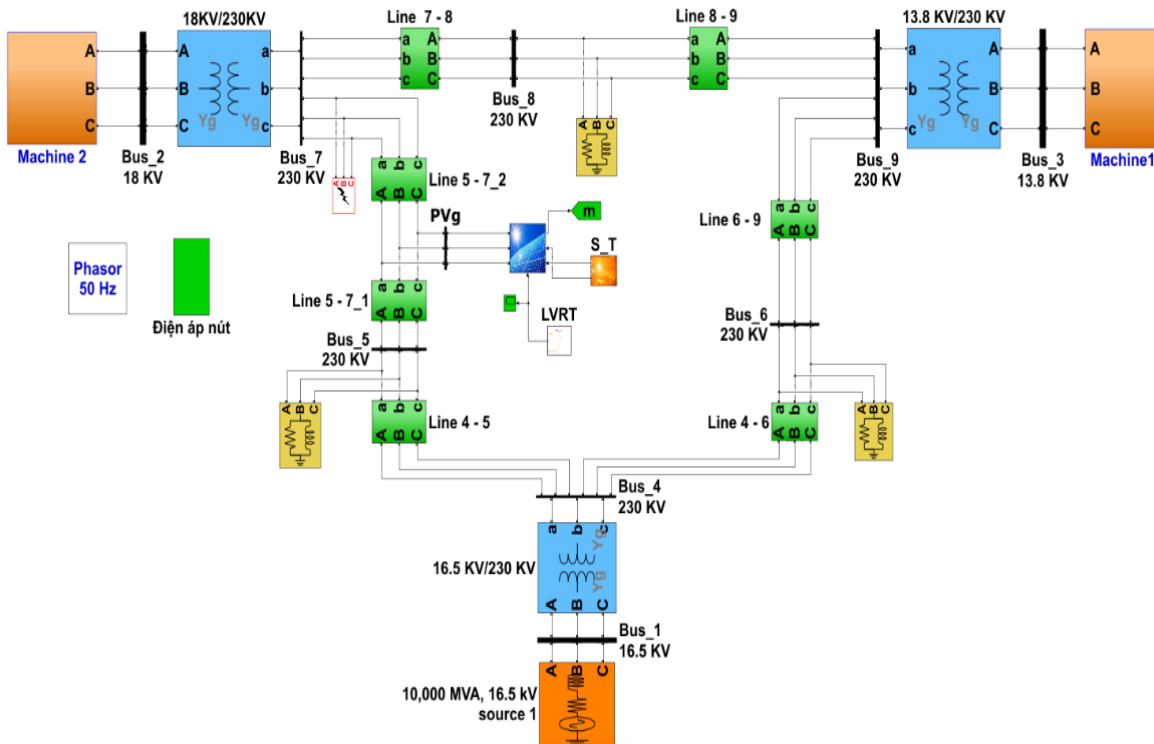


Fig. 11. PV model connected to 9-bus system

For each fault case, the bus voltages can cut LVRT characteristics at different moments. The simulation results are clearly shown in (Fig. 12 to Fig. 18). The two LVRT characteristics are compared in all fault cases (Fig. 12). In the first case, when the fault happens within 0.1s, the voltage curve doesn't cut both two LVRT characteristics. However, the fault happening within 0.2s has different results when considering the two characteristics, the IND-LVRT characteristic doesn't cut the voltage curve, while the VIE-LVRT characteristic cuts at 12.15s leading to the PV's disconnection. For faults within 0.3s and 0.4s, both characteristics cut the voltage curve, however, the time of PV system disconnection for each characteristic is changed. The VIE-LVRT cuts the voltage curve in the cases of fault which happens within 0.3s, 0.4s case at 12.15s (Fig. 15a, Fig.16a) and the IND-LVRT cuts more lately at 12.3027s and 12.4037s respectively (Fig. 15b, Fig. 16b). Different

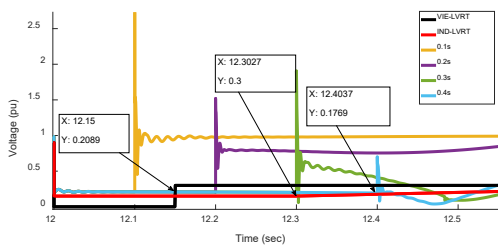
disconnection moments cause different impacts on power system. Bus voltages at each disconnection time have different oscillation magnitudes and durations. In the case of fault within 0.1s, both characteristics do not cut the voltage curve, so the influence between the two characteristics on the voltage of the buses has not been clear (Fig. 13). In the case of fault within 0.2s, there is a difference between the two characteristics: the VIE-LVRT cuts the voltage curve at 12.15s (Fig. 14a), causing a slight drop of voltage at all buses; while considering IND-LVRT, PV stays connected, so post-fault bus voltages have lower oscillation amplitudes and durations (Fig. 14b). For faults within 0.3s and 0.4s, both characteristics cut the voltage curve, for each disconnection moment, bus voltages also have the same value. When VIE-LVRT is used, bus voltages tend to fluctuate more strongly with higher amplitudes and require a longer stabilization time than when using the IND-LVRT.

The moment when PV is disconnected has a great impact on voltage stability in each fault case. For faults that happen within 0.1s and 0.2s, bus voltages stabilize after a short time. For the 0.3s fault case (Fig. 17), using the VIE-LVRT leads to voltage instability, however, when using IND-LVRT, the voltages are stable after a while. For the 0.4s fault case (Fig. 18), bus voltages all become unstable when using the two characteristics.

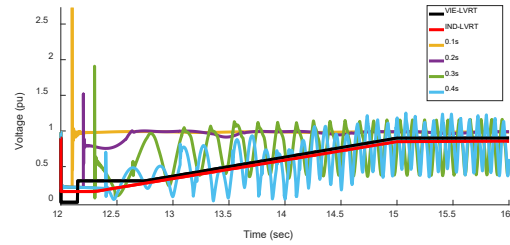
DC link voltage curves, representing the relationship between DC power and AC power, in cases considering the two LVRT characteristics are shown in Fig. 19 and Fig. 20. In Fig. 20, the voltage curves oscillate and return to steady state after clearing fault, the post-fault voltages have the same values as the pre-fault ones. Fig. 19 shows that transient voltage amplitudes, oscillation times in the two cases are different. The 0.1s voltage curve reaches the steady state faster but the transient voltage amplitude is higher

than the 0.2s IND-LVRT voltage curve. In Fig. 20, it is shown that the transient voltage amplitudes are much lower than those in the no PV's disconnection case, and at different disconnection moments, the transient voltage curves are different too. Excessively high transient voltage has bad impacts on the equipment and possibly destroys the whole PV system. Therefore, when the LVRT characteristic is applied, to find appropriate PV disconnection time, operators need to consider the DC link voltage, not just the voltage at the connection point.

When there is a disturbance if PV keeps staying connected for a long time, electrical and electronic equipment can be destroyed. However, when PV is disconnected, it will cause economic losses, and losing a source of power supply can lead to technical requirements violation. Therefore, there is a need to find a suitable characteristic for specific system.

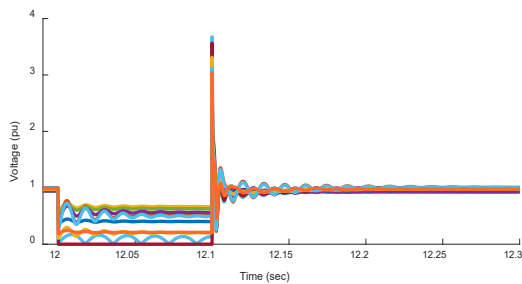


(a) Observation within 0.6s

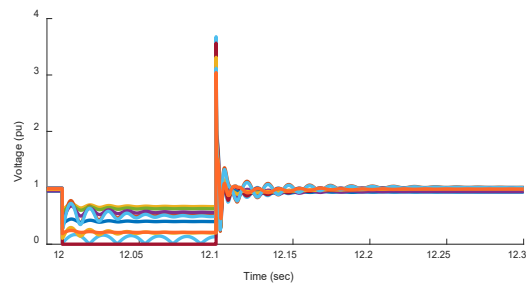


(b) Observation within 6s

Fig. 12. Bus voltage curves in all cases, without LVRT

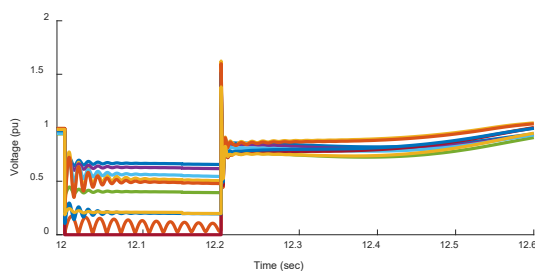


(a) Fault happens within 0.1s, VIE-LVRT

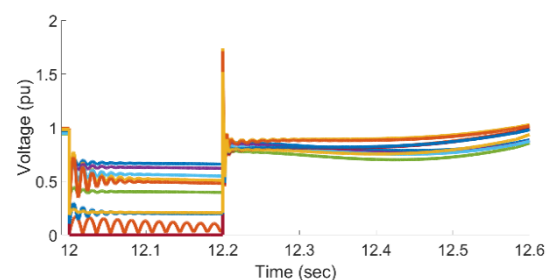


(b) Fault happens within 0.1s, IND-LVRT

Fig. 13. The LVRT characteristic and bus voltage curves in different fault cases

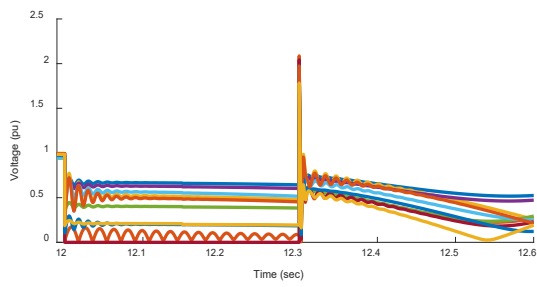


(a) Fault happens within 0.2s, VIE-LVRT

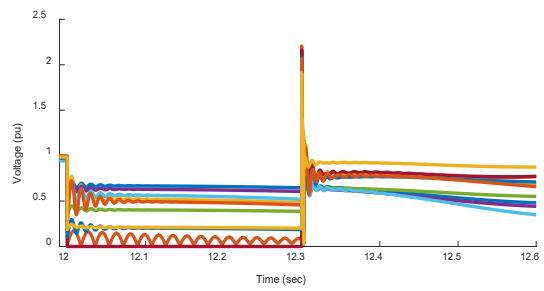


(b) Fault happens within 0.2s, IND-LVRT

Fig. 14. The LVRT characteristics and bus voltage curves in case of fault within 0.2s

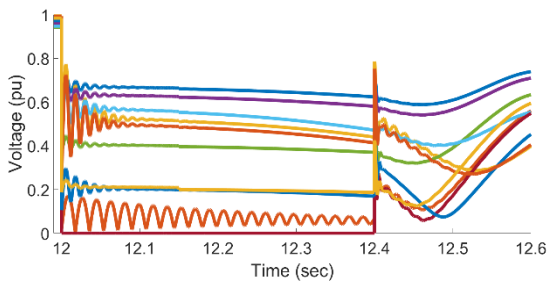


(a) Fault happens within 0.3s, VIE-LVRT

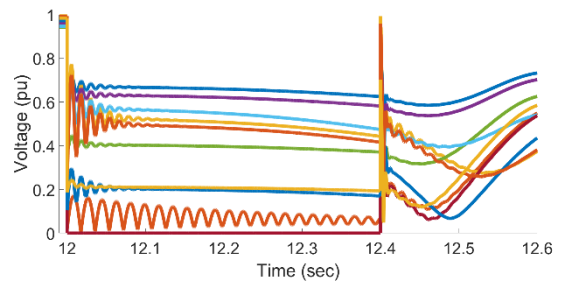


(b) Fault happens within 0.3s, IND-LVRT

Fig. 15. The LVRT characteristics and bus voltage curves in case of fault within 0.3s

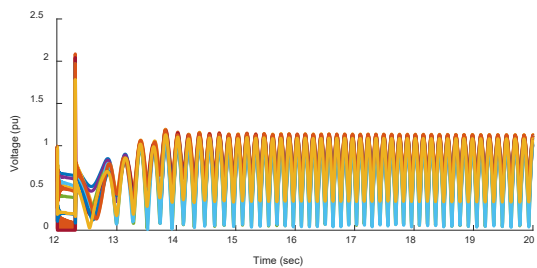


(a) Fault happens within 0.4s, VIE-LVRT

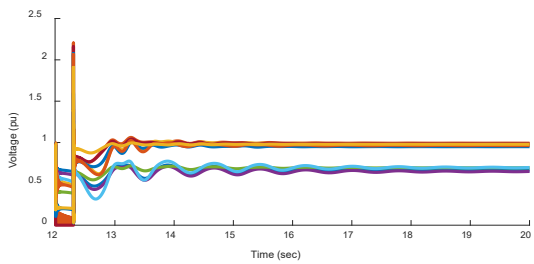


(b) Fault happens within 0.4s, IND-LVRT

Fig. 16. The LVRT characteristics and bus voltage curves in case of fault within 0.4s

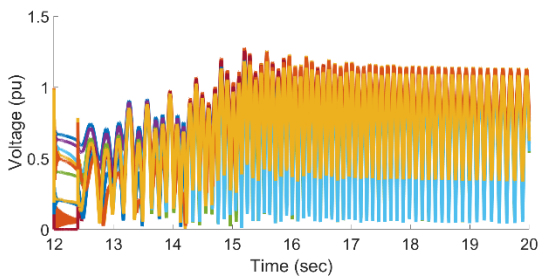


(a) Fault happens within 0.3s, VIE-LVRT

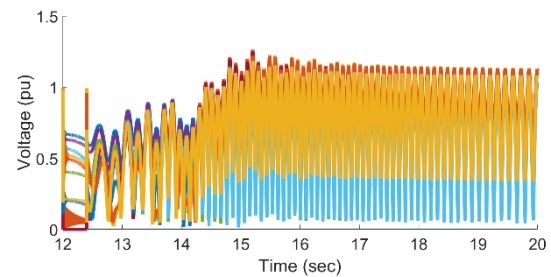


(b) Fault happens within 0.3s, IND-LVRT

Fig. 17. Zoomed in the LVRT characteristics and bus voltage curves in case of fault within 0.3s



(a) Fault happens within 0.4s, VIE-LVRT



(b) Fault happens within 0.4s, IND-LVRT

Fig. 18. Zoomed in the LVRT characteristics and bus voltage curves in case of fault within 0.4s

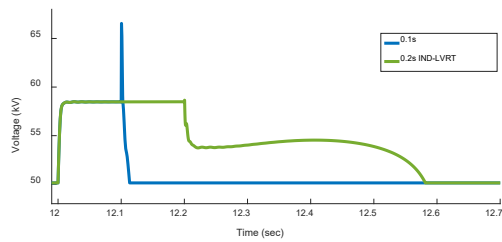


Fig. 19. DC link voltage in cases when PV isn't disconnected

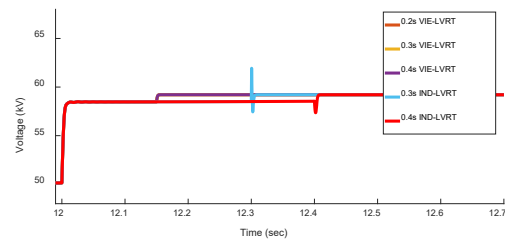


Fig. 20. DC link voltage in cases when PV is disconnected

One of the many advantages of using the proposed phasor model is the fast simulation speed. By comparison above IEEE 9-bus system with a system using the discrete PV model that is available in Simscape Power Systems Library of MATLAB R2020b, the results show that the system using PV phasor model has a much faster running simulation time than the other one. For example, under the same condition test on 01 computer, the system has PV phasor model takes 29.35s to complete 20s simulation with a three-phase fault within 0.2s while the other system takes 161.23s, although the utility grid of the second one is modeled simpler than the IEEE 3-machine system. It can be seen that the phasor model of the PV systems is better than discrete or continuous model in terms of simulation time.

5. Conclusion

This paper presents the dynamic phasor model of a large PV system in MATLAB/Simulink for voltage stability analysis as well as the influence of the LVRT characteristics of PV system on voltage stability under the disturbance condition. The proposed model can be used for power system stability analysis with fast and exact simulation. In the model of PV system, the LVRT characteristic can be adjusted easily which is useful to find an appropriate one to enhance power system stability. The results show that each LVRT characteristic has different effects on the voltage stability of the power system. Therefore, finding an LVRT characteristic of the PV system and control schemes to improve the system stability under different PV system capacities need to be more concerned.

Acknowledgments

This research is supported by the Ministry of Industry and Trade (MOIT) through the project ĐTKHCN.216/17 with Hanoi University of Science and Technology (HUST). The authors would like to thank MOIT and HUST for all support.

References

[1] S. M. Ismael, S.H.E. Aleem, A. Y. Abdelaziz, A. F. Zobaa, State-of-the-art of hosting capacity in modern power systems with distributed generation, *Renewable Energy*, vol. 130, pp. 1002-1020, Jan. 2019,

<https://doi.org/10.1016/j.renene.2018.07.008>.

[2] Nguyen Hoang Viet and A. Yokoyama, Impact of fault ride-through characteristics of high-penetration photovoltaic generation on transient stability, 2010 International Conference on Power System Technology, pp. 1-7, 2010, <https://doi.org/10.1109/POWERCON.2010.5666558>.

[3] M. Rosyadi, A. Umemura, R. Takahashi, J. Tamura, S. Kondo and K. Ide, Development of phasor type model of PMSG based wind farm for dynamic simulation analysis, 2015 IEEE Eindhoven PowerTech, pp. 1-6, 2015. <https://doi.org/10.1109/PTC.2015.7232485>.

[4] K. K. Gajjar and M. C. Chudasama, Dynamic phasor model of wams enabled transient stability controller, 2017 International Conference on Information, Communication, Instrumentation and Control (ICICIC), pp. 1-6, 2017 <https://doi.org/10.1109/ICOMICON.2017.8279048>.

[5] S. M. Kotian and K. N. Shubhanga, Dynamic phasor modelling and simulation, 2015 Annual IEEE India Conference (INDICON), pp. 1-6, 2015 <https://doi.org/10.1109/INDICON.2015.7443446>.

[6] S. Jahan, S.P. Biswas, M.K. Hosain, M.R. Islam, , S. Haq, A.Z. Kouzani, MAP. Mahmud, An advanced control technique for power quality improvement of grid-tied multilevel inverter, *Sustainability* 2021, vol. 13, no. 2, 2021 <https://doi.org/10.3390/su13020505>.

[7] S. Singer, B. Rozenshtein and S. Surazi, Characterization of PV array output using a small number of measured parameters, *Solar Energy*, vol. 32, pp. 603-607, 1984 [https://doi.org/10.1016/0038-092X\(84\)90136-1](https://doi.org/10.1016/0038-092X(84)90136-1).

[8] Y. Xie, J. Huang, X. Liu, F. Zhuo, B. Liu and H. Zhang, PV system modeling and a global-planning design for its controller parameters, 2014 IEEE Applied Power Electronics Conference and Exposition - APEC 2014, pp. 3132-3135, 2014, <https://doi.org/10.1109/APEC.2014.6803752>.

[9] A. Yazdani, R. Iravani, Voltage-sourced converters in power systems: modeling, control, and applications. New Jersey, USA: John Wiley & Sons, 2010, pp. 127–244.

[10] F. Blaabjerg, D. M. Ionel, Renewable Energy Devices and Systems with Simulations in MATLAB and ANSYS. Florida, USA: CRC Press, 2017, pp. 67–90.

- [11] V. Blasko and V. Kaura, A novel control to actively damp resonance in input LC filter of a three-phase voltage source converter, *IEEE Transactions on Industry Applications*, vol. 33, no. 2, pp. 542-550, Apr. 1997
<https://doi.org/10.1109/28.568021>.
- [12] C. Du, M. H. J. Bollen, E. Agneholm and A. Sannino, A New Control Strategy of a VSC–HVDC System for High-Quality Supply of Industrial Plants, *IEEE Transactions on Power Delivery*, vol. 22, no. 4, pp. 2386-2394, Oct. 2007
<https://doi.org/10.1109/TPWRD.2007.899622>.
- [13] Y. Yang, K. A. Kim, F. Blaabjerg, A. Sangwongwanich, *Advances in Grid-Connected Photovoltaic Power Conversion Systems*. Cambridge, UK: Woodhead Publishing, 2019
- [14] Circular No. 30/2019/TT-BCT, Electricity Regulatory Authority of Vietnam, Vietnam, 2019.